Large-Scale Mapping of Transposable Element Insertion Sites Using Digital Encoding of Sample Identity

Daryl M. Gohl,*[,1] Limor Freifeld,[†,‡,1] Marion Silies,* Jennifer J. Hwa,* Mark Horowitz,[†] and Thomas R. Clandinin*[,2]

*Department of Neurobiology and [†]Electrical Engineering, Stanford University, Stanford, California 94305, and [‡]Department of Electrical Engineering and Computer Science, Massachusetts Institute of Technology, Cambridge, Massachusetts 02139

ABSTRACT Determining the genomic locations of transposable elements is a common experimental goal. When mapping large collections of transposon insertions, individualized amplification and sequencing is both time consuming and costly. We describe an approach in which large numbers of insertion lines can be simultaneously mapped in a single DNA sequencing reaction by using digital error-correcting codes to encode line identity in a unique set of barcoded pools.

NEXT-generation sequencing (NGS) technologies have greatly reduced the cost of DNA sequence analysis through the parallel sequencing of many short fragments. However, many applications, including molecular cloning and mutational analysis continue to rely on conventional capillary electrophoresis Sanger sequencing methods, as these are well-suited to sequencing individual fragments. Thus, one challenge in using NGS technologies in such applications lies in preserving sample identity while sequencing many samples simultaneously. This challenge can be addressed by encoding sample identity through either DNA barcoding or directed pooling (Mazurkiewicz *et al.* 2006; Erlich *et al.* 2009; Goodman *et al.* 2009; Prabhu and Pe'er 2009).

Transposable elements represent powerful tools for manipulating the genomes of many model organisms (Bellen *et al.* 2011; Bire and Rouleux-Bonnin 2012). Thus, determining the genomic location of transposon insertion sites is a common experimental goal. Several methods, such as inverse PCR and splinkerette PCR, are used to amplify a short fragment of the genome directly adjacent to an insertion (Ochman *et al.* 1988; Devon *et al.* 1995). Subsequently, capillary electrophoresis Sanger sequencing is used to sequence each amplicon. As a result, all processing reactions must be performed independently on each sample, making the cost and labor associated with mapping collections of thousands of insertion lines significant. Several techniques have used NGS to map transposons in large populations of bacteria or yeast (Goodman *et al.* 2009; Uren *et al.* 2009; Iskow *et al.* 2010; Febrer *et al.* 2011). However, most of these approaches do not allow the insertion site to be associated with the identity of the original sample.

While DNA barcoding can be used to encode sample identity prior to NGS, adding the barcode requires either individualized molecular manipulation of each sample or prior construction of a sequence-tagged transposon library (Mazurkiewicz *et al.* 2006; Hamady *et al.* 2008). As an alternative, pooling strategies can be used to encode sample identity, and several recent studies have reported strategies for efficient, error-resistant encoding in pooled DNA samples (Erlich *et al.* 2009; Goodman *et al.* 2009; Prabhu and Pe'er 2009). However, none of these approaches have been applied to the large genomes of multicellular eukaryotes, which present unique challenges due to repetitive sequences, increased sequence complexity, and an ~100- to 1000-fold reduction in the ratio of transposon sequence to genome sequence.

We have developed a method for mapping transposons in multicellular eukaryotes that allows large numbers of transposon inserts to be mapped in a single NGS reaction (Figure 1A). This

doi: 10.1534/genetics.113.159483
Manuscript received November 8, 2013; accepted for publication December 21, 2013; published Early Online December 27, 2013.
Supporting information is available online at http://www.genetics.org/lookup/suppl/doi:10.1534/genetics.113.159483/-/DC1.
[1]These authors contributed equally to this work.
[2]Corresponding author: Department of Neurobiology, Stanford University, 299 West Campus Dr., Stanford, CA 94305. E-mail: trc@stanford.edu

method makes use of a pooling strategy that encodes sample identity using error-correcting Hamming codes (Hamming 1950). Hamming codes make use of a small number of additional bits of information, so-called parity bits, to detect and correct errors. The error detecting and correcting capacity of Hamming codes and other error-correction codes, such as the Golay code (Golay 1949), depend upon the Hamming distance between code words (messages), a reflection of the number of parity bits used. The Hamming distance is defined as the number of changes in a binary sequence that would be necessary to change one code word into another code word. As such, if an estimate of the expected error rate in a pooled mapping experiment can be made, an error correcting code with sufficient detection and correction capabilities can be matched to this expected noise. The method we describe further enables the incorporation of additional error-correcting steps and associates a quantitative measure of confidence with each decoding. This strategy greatly reduces the cost associated with mapping libraries of insertions compared to the widely used conventional methods.

Materials and Methods

Hamming encoding of sample identity

A collection of 1065 *piggyBac* transposon insertion lines was generated as previously described (Gohl *et al.* 2011; Silies *et al.* 2013). Of these, 126 lines were inserted on the 1st chromosome, 351 lines were inserted on the 2nd chromosome, 584 lines were inserted on the 3rd chromosome, and 4 lines were inserted on the 4th chromosome. Since the insertion chromosome was known for each line, codes were selected for each of these populations independently (allowing the use of the same code words for lines in which the insertions were on different chromosomes). To encode at least 584 lines, a minimum of 10 data bits are required. For each line with an insertion in a particular chromosome, we assigned a unique 11-bit binary identification (ID) number. Since line numbers require no more than 10-bit encoding, parity bits were included in these IDs. The ID numbers were then encoded as 15-bit Hamming code words. This encoding guarantees a minimal Hamming distance of at least 3 bits between code words and thus enables correcting single bit errors (if a single bit error occurs, there is only one valid code word at a Hamming distance of 1 from the error-containing 15-bit sequence). All code for encoding and decoding and subsequently described analysis was written in Matlab (Mathworks, Natick, MA).

A single fly was allocated to the specified subset of the 15 pools for each line. DNA was isolated from each pool by grinding the flies in 2.75 ml of lysis buffer (0.1 M Tris pH 8.0, 0.4 M NaCl, 25 mM EDTA, 1% SDS) on ice, adding 2.75 ml of Tris-buffered phenol (Invitrogen, Carlsbad, CA), and then extracting three times with 2 ml of 25:24:1 phenol:chloroform: isoamyl alcohol (IAA) (Invitrogen). The resulting sample was extracted once with 2 ml of chloroform (EM Science, Gibbstown, NJ) and 1.2 ml of the aqueous phase was precipitated with 4 ml of >99.5% ethanol (Sigma-Aldrich, St. Louis) and placed in the freezer for 30 min. The sample was then centrifuged for 10 min at 13,200 relative centrifugal force and the resulting pellet was washed twice with 0.5 ml of 70% ethanol and allowed to air dry for 10 min. The pellet was resuspended in 1 ml of distilled water (dH_2O).

Library preparation and validation

A total of 200 ng of each of the 15 pooled DNA samples was sheared to an average size of 200 bp using a Covaris S2 ultrasonicator (Covaris, Woburn, MA). Shearing was confirmed using an Agilent Bioanalyzer High-Sensitivity chip (Agilent, Santa Clara, CA). The sheared DNA was end repaired and Illumina-compatible adapters were added following the protocol described by Meyer and Kircher (2010). A total of 50 μl (50–150 ng) of sheared DNA was incubated together with 7 μl T4 ligase buffer [New England Biolabs (NEB), Ipswich, MA], 0.28 μl 25 mM dNTP mix (Invitrogen), 0.7 μl 100 mM dATP (Invitrogen), 3.5 μl T4 polynucleotide kinase (NEB), 1.4 μl T4 DNA polymerase (NEB), and 7.12 μl dH_2O for 15 min at 25°, followed by 5 min at 12°. End-repaired DNA was purified using 1.8× Agencourt AMPure XP beads (Beckman-Coulter, Danvers, MA) and resuspended in 20 μl elution buffer (EB) (10 mM Tris-Cl, pH 8.0; Qiagen, Valencia, CA). Next, adapters were prepared as follows: 40 μl of 500 μM IS1_adapter.P5 and IS3_adapter.P5+P7 oligos and IS2_adapter.P7 and IS3_adapter.P5+P7 oligos (Supporting Information, Table S1), and annealed in a 100-μl reaction with 10 μl of 10× hybridization buffer (500 mM NaCl, 10 mM Tris-Cl, pH 8.0, 1 mM EDTA, pH 8.0), by heating to 95° and ramping to 12° at 0.1°/sec in a thermal cycler. The annealed adapters were mixed together and 1 μl of adapter mix was added to 20 μl of end-repaired DNA, together with 4 μl T4 ligase buffer, 1 μl T4 DNA ligase (NEB), and 14 μl dH_2O and incubated at 22° for 30 min. Adapter-ligated DNA was purified using 1.8× Agencourt AMPure XP beads and resuspended in 20 μl EB. Next, adapters were filled in by incubating 20 μl of purified, adapter-ligated DNA with 4 μl Thermopol reaction buffer (NEB), 0.4 μl 25 mM dNTP mix, 1.5 μl Bst large fragment DNA polymerase (NEB), and 14.1 μl dH_2O at 37° for 20 min. The resulting DNA was purified using 1.8× Agencourt AMPure XP beads and resuspended in 20 μl EB.

Ligation of adapter molecules was confirmed using an Agilent Bioanalyzer High-Sensitivity chip. To test whether specific transposon lines were present in the appropriate adapter-ligated pooled libraries, 1 μl of DNA from each library was amplified using GoTaq (Promega, Madison, WI) with a primer specific to the 5′ end of the *piggyBac* transposon, 5prPBacPooltest_For (Table S1) and a primer specific to the flanking genomic region of a particular line (0359_5prRev, 0606_5prRev, or 0754_5prRev, Table S1) as determined by splinkerette PCR. Splinkerette mapping of individual *piggyBac* transposon inserts was carried out as previously described (Potter and Luo 2010) (see Table S1 for primer sequences and File S1 and File S2 for sequence data).

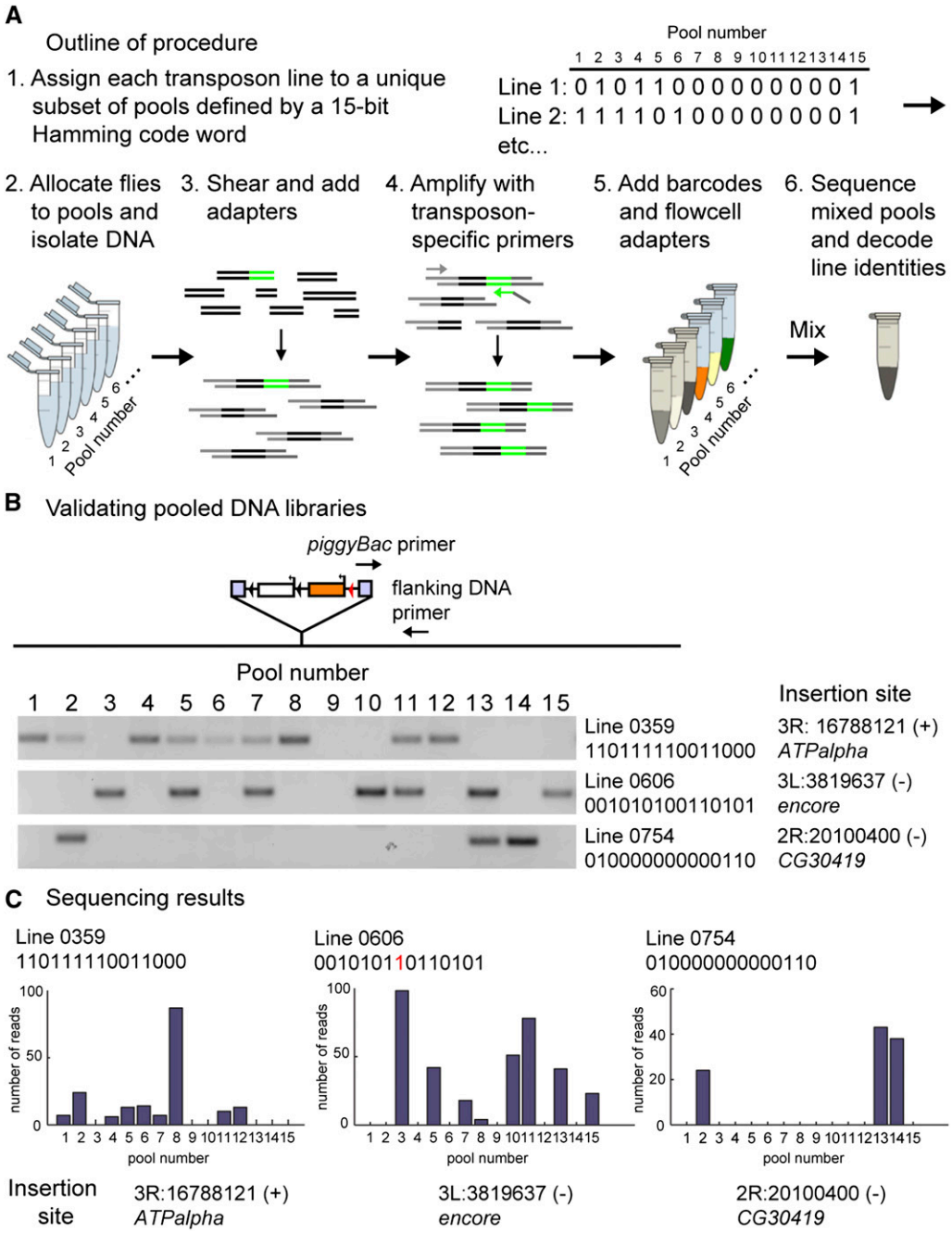

Figure 1 Outline of the method and examples of resulting data. (a) Outline of the method used for multiplexed mapping of large numbers of transposon insertion lines. (b) Amplified DNA from the transposon–genome junction for three representative inserts. Line identities could be correctly decoded from the pooled samples. (c) Illumina sequencing data from pooled samples for 5′ end-associated sequences for the same three lines shown in b. These three lines were correctly decoded and matched the genomic positions determined by splinkerette PCR mapping. The sequences associated with lines 0359 (inserted in *ATPalpha*) and 0754 (inserted in *CG30419*) were decoded without any error correction, and the sequence associated with line 0606 (inserted in *encore*) was decoded with a 1 to 0 correction. The error is denoted by a red digit.

Transposon enrichment and DNA sequencing

To amplify *piggyBac* transposon sequences from the pooled libraries, primers were designed that had homology to the 5′ or 3′ ends of the *piggyBac* transposon and also contained the p7 end Illumina adapter sequence (pBac5_sr_adapt and pBac3_sr_adapt; Table S1). The 5′ and 3′ transposon ends were separately amplified from each of the 15 pools for 25 cycles using Phusion polymerase (Thermo Scientific, Wilmington, DE) with either the pBac5_sr_adapt or pBac3_sr_adapt primer and the IS4_indPCR.P5 primer. To minimize amplification artifacts, two independent PCR reactions were set up for each sample and pooled prior to purification using the MinElute PCR purification kit (Qiagen). Samples were resuspended in 20 μl of EB. Indices (DNA barcodes) and Illumina flow cell adapters were added with a second round of PCR. Each sample was amplified for 10 cycles using the IS5_reamp.P5 primer (Table S1) and one of the 30 indexing primers (indexing 1–15 primers were used for the amplified 5′ end sequences and indexing 16–30 primers were used for the amplified 3′ end sequences; Table S1). As with the first round of PCR, two independent PCR reactions were set up for each sample and pooled prior to purification using the MinElute PCR purification kit. Samples were resuspended in 20 μl of EB. Concentrations for all 30 samples were quantified using a NanoDrop (Thermo Scientific) and mixed in equal concentrations to make a final pooled sample for sequencing.

Table 1 Accuracy of the original lists and best score lists compared to splinkerette mapping

		Comparison to reference set		Comparison to validation set		Total	
	No. unique lines	No. correct (%)	No. incorrect (%)	No. correct (%)	No. incorrect (%)	No. correct (%)	No. incorrect (%)
Original lists							
Direct decoding 5′ positions	863	56/89 (62.9)	33/89 (37.1)	15/38 (39.5)	23/38 (60.5)	71/127 (55.9)	56/127 (44.1)
Direct decoding 3′ positions	915	56/103 (54.4)	47/103 (45.6)	13/53 (24.5)	40/53 (75.5)	69/156 (44.2)	87/156 (55.8)
Best score lists							
Best 5′ position by score	863	54/57 (94.7)	3/57 (5.3)	14/21 (66.7)	7/21 (33.3)	68/78 (87.2)	10/78 (12.8)
Best 3′ position by score	915	53/57 (93.0)	4/57 (7.0)	11/25 (44.0)	14/25 (56.0)	64/82 (78.0)	18/82 (22.0)
5′ and 3′ agreement	755	48/48 (100.0)	0/48 (0.0)	1/1 (100.0)	0/1 (0.0)	49/49 (100.0)	0/49 (0.0)

Numbers and percentages of correct and incorrect mapping suggestions on each list are shown in comparison to an initial reference set that was used to optimize the decoding procedure, and to an additional validation set. Both of these sets comprised map positions determined by splinkerette PCR. Generation of the two original lists and the three best score lists are described in the main text and *Materials and Methods*. The original lists contained multiple line suggestions for some positions and multiple position suggestions for some lines. The number of unique lines represented on each list is shown.

The amount of enrichment of transposon sequences relative to genomic loci was determined by comparing amplification with a primer set specific to the *piggyBac* 5′ end (PB5′ qPCR forward/PB5′ qPCR reverse) and a primer set specific to the *apterous* gene (ap qPCR forward/ap qPCR reverse). A total of 30 μl of this mixed sample was purified using 1.8× Agencourt AMPure XP beads to remove primers and the concentration of this sample was measured using an Agilent Bioanalyzer High-Sensitivity chip. The resulting sample was sequenced to generate paired-end 150-bp reads using a MiSeq Benchtop sequencer (Illumina, San Diego).

Data analysis

The process by which insertion positions were assigned can be divided into two parts: first, reads were processed and mapped to chromosomes; second, read positions were assembled into codes and associated with the corresponding line.

Preprocessing of sequenced reads and mapping to the Drosophila genome

First, sequence reads with many undetermined base pairs were edited to remove the portion that failed to sequence. Next, sequences were filtered by whether they contained the transposon sequences associated with the 5′ and 3′ ends using Matlab's built-in implementation of Barton's local alignment algorithm (Barton 1993). The transposon reference sequences are as follows:

piggyBac 3′ end: CGTACGTCACAATATGATTATCTTTCTAGGGTT**AA**

piggyBac 5′ end: GCATGCGTCAATTTTACGCAGACTATCT**TTCTAGGGTTAA.**

Alignments were considered successful if the transposon reference sequence aligned to the beginning of the read, the alignment score was >15, the alignment length was equal to the reference sequence length, and a perfect match was found to a 2-bp sequence at the end of the 3′ end transposon reference sequence and a 12-bp sequence at the end of the 5′ end transposon reference sequence (boldface text above, see Figure S1). These final sequences were absent from the amplification primers and thus were useful in distinguishing true transposon-containing reads from off-target amplification events. Because this signature sequence was longer for the 5′ end of the transposon, we were able to select 5′ *piggyBac*-containing reads with higher confidence than 3′ *piggyBac*-containing reads. If a reference transposon sequence was identified in a read, it was removed prior to subsequent analysis; otherwise the read was discarded.

In reads that contained the reference transposon sequence we also looked for the Illumina p5 adapter sequence using the same local alignment algorithm as described above: p5 side Illumina adapter: AGATCGGAAGAGCGTCGTGTAGGGAAAGAGTGTAGATCTCGGTGGTCGCCGTATCATT. We defined an alignment to the adapter reference sequence as correct if the alignment score was >15 and encompassed the entire reference sequence or if the alignment score was >10 and the alignment was to the end of the sequenced read. If the adapter sequence was identified in a read sequence, it was removed from subsequent analysis.

Following removal of transposon reference sequences and Illumina adapter sequences (if found), each read was mapped to the *Drosophila melanogaster* FlyBase r5.22 reference genome using Bowtie, a fast, memory-efficient short-read aligner (Langmead *et al.* 2009). A single best alignment was used for subsequent analysis and was considered to define the position in the genome to which the read mapped (representing a position near a transposon insertion site).

Associating putative transposon insertion positions with lines

The 3′ and 5′ end reads were processed separately. We first identified positions that had many sequencing reads associated with them and thus were likely to represent an insertion position. Only reads longer than 12 bp were considered. For 5′ end reads, we required 5 or more reads to map to a position for it to be considered as a putative insertion position. For 3′ end sequenced reads, we required 25 or more sequence reads to map to a position. For every position considered as a potential insertion position, the following procedure was applied to derive a line assignment: first, a 15-bit-long digital sequence, representing the presence ("1" bit) or absence ("0" bit) of reads from each of the 15 pools, was generated. We then decoded this sequence using the Hamming code to

find a corresponding line ID (Table S2)—this procedure allows correction of a single error in the digital sequence with respect to the code word associated with the corresponding line. If the decoded message was indeed a line ID, we also checked whether the chromosome containing the sequenced reads matched the annotated chromosome of insertion for the line. Decoded identities corresponding to a line with an incorrect chromosome assignment were kept for subsequent analysis. Decoded identities corresponding to a correct chromosome assignment were considered as potentially correct (but see additional validation steps below). In addition, we generated a second digital sequence for each putative insertion position by requiring reads from a particular pool to represent a distribution of lengths with more than one length so as to ensure independence. Thus, if all reads from a particular pool had the same length, the bit corresponding to this pool was set to 0 rather than to 1 in this alternate code. This 15-bit code word was also decoded using the Hamming code as described above and the resulting decoding was assigned to either the incorrect chromosome list or the potentially correct line assignment list.

The resulting list of assignments of lines to insertion positions consisted of both multiple position suggestions for the same line and multiple line assignments to the same position. In addition, there was significant overlap between the 3′ and 5′ end lists. We therefore derived multiple procedures for attributing confidence levels for suggested position-line pairings as well as for extracting a single insertion position assignment for each line.

First, since 3′ and 5′ end sequences represent completely separate amplification and processing, lines that were assigned the same insertion position in both lists were likely to be correctly assigned. Thus, we used the list of lines that mapped to the same insertion position based on 3′ end reads and 5′ end reads to compute metrics by which confidence could be deduced for other lines that were not included in this list. The following characteristics were used for confidence assignment:

(1) The number of reads that mapped to the putative insertion position and used for generating the digital code.
(2) The distance between the digital sequence representing the presence or absence of reads mapping to the current position in each of the 15 pools and the Hamming code for the line. This distance is 1 for line assignments reflecting Hamming decoding corrections but can be larger when pools with reads of a unique length are assigned 0s.
(3) The difference between the mean number of unique read lengths in pools assigned a 1 in the code word associated with the assigned line and the mean number of unique read lengths in pools assigned a 0 in the code word associated with the assigned line.
(4) The difference between the mean number of reads in pools assigned a 1 in the code word associated with the assigned line and the mean number of reads in pools assigned a 0 in the code word associated with the assigned line.
(5) The mean length of reads that mapped to the position associated with the line.
(6) The number of pools represented by a 1 bit in the code word associated with the line in which the number of unique read lengths is one.

We refer to these parameters as the "agreement-based clean-up parameters." For each of these parameters, we determined the minimal or maximal value (depending on which represents lower confidence) represented in the list of lines that decoded in the same manner using 3′ end reads and 5′ end reads. We then examined other lists (see below) by requiring that suggested decodings be associated with parameter values that are not worse than the worst parameter value identified in the corresponding (3′ end or 5′ end) agreement list. The lists of suggested decodings based on 3′ end reads and on 5′ end reads were then screened according to this criterion. Next, we extracted a single suggestion for each line on these lists by selecting the decoding that had a maximal difference between the mean number of unique lengths of reads in pools assigned a 1 in the code word associated with the line and the mean number of unique lengths of reads in pools assigned a 0 in the code word associated with the line (parameter 3 above). If, however, this suggested decoding had a nonspecific chromosome assignment and a suggested decoding for the line existed that had a specific chromosome assignment, the decoding associated with the specific chromosome assignment was preferred even if it had a lower score.

We next compared these lists and extracted lists of suggested decodings that were in agreement (lines assigned to the same position), lists of lines that were in disagreement (lines assigned to different positions), and lists of lines that were only included in one of the lists (3′ end or 5′ end sequenced reads). This comparison implied different confidence levels for the lines appearing in different lists. Since 5′ suggestions were generally more reliable than 3′ suggestions, in cases where the 5′ and 3′ suggestions disagreed, only 5′ suggestions were retained.

Finally, we attempted to derive additional decoding suggestions for putative insertion positions that were not successfully assigned by the above described procedures: *i.e.*, suggested decodings associated with incorrect chromosomes or suggested decodings with line assignments where a better assignment was found for the same line. To do so, we considered lines in the final agreement lists between 3′ end and 5′ end sequences as correctly assigned lines and attempted to match putative insertion positions to the remaining lines by applying two different procedures:

(1) For putative insertion positions consisting of reads in a set of pools representing a subset of the pools associated with an unassigned line, the corresponding unassigned line was suggested as a decoding. In this manner, a "multiple zero-to-one error list" was generated.
(2) For putative insertion positions consisting of reads from all pools associated with the lines mapped to the putative

positions together with additional reads from other pools, the corresponding unassigned line was suggested as a decoding. In this manner, a "multiple one-to-zero error list" was generated.

The above described lists were further cleaned using the same agreement-based clean-up criteria described above. Furthermore, we compared the 3′ end and 5′ end versions of these lists to each other and to previously generated lists to search for matches to increase confidence in particular suggested decodings.

Code

Matlab code for Hamming encoding of line identities and decoding peaks of mapped reads is available for download at: http://www.stanford.edu/group/clandininlab/hamming.

Results

We tested our method on a collection of 1065 transposon insertion lines in *Drosophila*, generated using a *piggyBac* element (Gohl *et al.* 2011; Silies *et al.* 2013). Within this collection, the vast majority of strains contained a single insertion into the genome. Insertion strains were first grouped by the targeted chromosome (determined during strain construction) and then each line on a given chromosome was assigned a unique ID number. Next, each ID number was encoded as a 15-bit binary Hamming "code word." The use of 15-bit code words, as opposed to the 11 bits that would be the minimum necessary for representing 1065 lines, allowed us to create distance between code words such that at least three errors would be needed to convert one code word into another. Specifically, using a Hamming code, we guaranteed this separation between all code words, enabling the detection of up to two errors and correction of single errors (Hamming 1950). Each of the 15 bits represented a pool of animals. Animals from a specific line were added to each pool corresponding to a digital 1 in the code word encoding the line ID and were not added into pools corresponding to digital 0s. Next, genomic DNA was extracted from each pool, mechanically sheared to an average fragment size of 200 bp, and attached to Illumina adapters (Meyer and Kircher 2010). To verify the distribution of sample DNA within the correct subset of pools, we designed primers to amplify several insertions that had previously been mapped using conventional splinkerette PCR (Potter and Luo 2010). For each of these, the predicted PCR products were observed in the anticipated subset of pools (Figure 1B). Transposon sequences in each pool were then amplified using hemi-specific PCR using one primer in the transposon and one primer in the Illumina adapter. Pool-specific DNA barcodes and flow cell adapters were then added using another round of PCR amplification. Next, DNA from the individual, barcoded pools was mixed and sequenced in a single 150-bp, paired-end MiSeq run (Bentley *et al.* 2008). Using the barcode information, sequence reads were divided by the pools from which the DNA samples were extracted.

Prior to generating a list of putative insertion sites, the following processing steps were performed. First, sequence reads for each pool were filtered by whether they contained *piggyBac* transposon sequence and trimmed to remove transposon and adapter sequences. Then, sequences were mapped to the genome using the short-read alignment program, Bowtie (see *Materials and Methods* for details) (Langmead *et al.* 2009). Next, we generated lists of suggested line identities for insertion positions for both the 5′ and 3′ transposon junctions (which were amplified and barcoded in independent reactions). To do this, we first identified putative transposon insertion sites, positions in the genome to which many reads mapped. Then, we inferred line identity corresponding to each position based on the digital sequence defined by the presence or absence of sequencing leads mapped to this position across the 15 pools (Figure 1C). Because the DNA samples were mechanically sheared, independent reads from the same pool should vary in length. We therefore also attempted to assign a second suggested code word for each position by flipping 1 bits to 0 bits when the corresponding pools only contained reads of a single length, meaning that the putative insertion site had only been identified once. Finally, these digital sequences, of which there were either one or two for every position, were decoded to retrieve the line IDs from the corresponding code words. At this point, corrections based on the Hamming code were made. Since we knew the insertion chromosome for each line, we excluded mapping suggestions that pointed to an incorrect chromosome and set these aside for subsequent analysis (see below). In sum, following all data processing steps above, each position was associated with either one or two suggested lines, thereby generating a comprehensive list of possible map position assignments.

Previous implementations of similar encoding strategies in prokaryotes relied solely on such direct decoding of sample IDs (Goodman *et al.* 2009). To characterize the performance of this decoding strategy, we used a reference set of internal controls consisting of the locations of 66 transposon insertions mapped using splinkerette PCR (File S1). Using 5′ end sequences, the initial list comprised suggested insertion positions for 863/1065 lines (81.0% of the collection); similarly, for the 3′ end sequences, 915/1065 lines (85.9% of the collection) were represented. In aggregate, these lists captured 958/1065 (90.0%) of the lines in the entire collection. However, both lists contained multiple suggested insertion positions for the same lines as well as multiple line suggestions for the same insertion position. Therefore, many of these suggestions were erroneous. Indeed, for 5′ end sequences, while correct positions were suggested for 56/57 lines from the reference set (and no positions were suggested for 9 lines in this set), 33 additional positions were incorrectly suggested for these lines. Thus, only 56/89 (62.9%) of all suggested positions for lines in the reference set were correct. Similarly, for 3′ end sequences, the fraction of incorrect suggestions was larger, with correct suggestions made for 56/57 lines in the reference set, but only 56/103 (54.4%) of all

Table 2 Accuracy of cleaned lists compared to splinkerette mapping

List ID	Cleaned lists	No. unique lines	Comparison to reference set		Comparison to validation set		Total	
			No. correct (%)	No. incorrect (%)	No. correct (%)	No. incorrect (%)	No. correct (%)	No. incorrect (%)
1	5′ and 3′ agreement	761	49/49 (100.0)	0/49 (0.0)	1/1 (100.0)	0/1 (0.0)	50/50 (100.0)	0/0 (0.0)
2	5′ and 3′ disagreement	40	3/3 (100.0)	0/3 (0.0)	6/10 (60.0)	4/10 (40.0)	9/13 (69.2)	4/13 (30.8)
3	Appears on 5′ list only	40	3/3 (100.0)	0/3 (0.0)	7/8 (87.5)	1/8 (12.5)	10/11 (90.9)	1/11 (9.1)
4	Appears on 3′ list only	99	4/4 (100.0)	0/4 (0.0)	7/10 (70.0)	3/10 (30.0)	11/14 (78.6)	3/14 (21.4)
5	5′ multiple 0-to-1 corrections	51	2/5 (40.0)	3/5 (60.0)	5/9 (55.6)	4/9 (44.4)	7/14 (50.0)	7/14 (50.0)
6	5′ multiple 1-to-0 corrections	188	0/11 (0.0)	11/11 (100.0)	11/30 (36.7)	19/30 (63.3)	11/41 (26.8)	30/41 (73.2)
7	3′ multiple 0-to-1 corrections	91	2/5 (40.0)	3/5 (60.0)	2/5 (40.0)	3/5 (60.0)	4/10 (40.0)	6/10 (60.0)
8	3′ multiple 1-to-0 corrections	283	1/14 (7.1)	13/14 (92.9)	18/48 (37.5)	30/48 (62.5)	19/62 (30.6)	43/62 (69.4)
9	5′ chromosome error	26	0/1 (0.0)	1/1 (100.0)	4/5 (80.0)	1/5 (20.0)	4/6 (66.7)	2/6 (33.3)
10	3′ chromosome error	53	0/4 (0.0)	4/4 (100.0)	4/8 (50.0)	4/8 (50.0)	4/12 (33.3)	8/12 (66.7)

Numbers and percentages of correct and incorrect mapping suggestions on each list are shown in comparison to an initial reference set that was used to optimize the decoding procedure, and to an additional validation set. Both of these sets comprised map positions determined by splinkerette PCR. Generation of the 10 cleaned lists is described in the main text and *Materials and Methods*. The list ID column corresponds to the list ID column in Table S3. The 5′ and 3′ disagreement list corresponds to lines that had different suggested mapping positions on the 5′ and 3′ cleaned lists. Since the 5′ mapping suggestions were generally more reliable than the 3′ suggestions, the numbers on this list and their positions (in Table S3) refer only to the 5′ list data.

suggested positions were correct (see "Original lists," Table 1). Thus, direct decoding was insufficient to reliably map lines.

To extract more accurate lists, consisting of single insertion suggestions for each line, we derived a score to capture the confidence in the match between the reads associated with a position and the corresponding line. This score was designed to reflect the fact that a large number of different read lengths associated with a specific position in a particular pool indicated a higher likelihood that the corresponding insertion was truly in that pool. We therefore calculated the difference between the mean number of unique read lengths found in pools assigned 1s in a given code and the mean number of unique read lengths in pools assigned 0s. We then selected the highest scoring single insertion position for each line and discarded all other suggested positions. Using this approach we generated very accurate lists with significantly fewer erroneous map position suggestions. In particular, the lists derived from 5′ and 3′ end sequences consisted of 54/57 (94.7%) and 53/57 (93%) correct insertion position suggestions for lines in the reference set, respectively (see "Best score lists," Table 1). As expected, there was substantial overlap and agreement between these two lists, with 755/1065 (70.1%) of lines having the same suggested position for both the 5′ and 3′ end decodings. This "agreement" list was perfectly accurate when compared to the reference list, as 48/48 (100%) of the reference insertions were correctly mapped (Table 1).

Since this agreement list was highly reliable, we used it to characterize the properties of insertion position - line assignment pairings that were indicative of accuracy. From this, we derived additional criteria to eliminate inaccurate mapping suggestions (see *Materials and Methods* for details). When these criteria were applied to the original direct decoding lists, 841/1065 (79.0%) of lines were represented in the cleaned 5′ list, 900/1065 (84.5%) of lines were represented in the cleaned 3′ list, and 761/1065 (71.5%) were on the agreement list (Table 2). These new lists correctly captured 55/55 (100%; 5′ end) and 53/56 (94.6%; 3′ end) of the lines in the reference set (data not shown).

To increase the fraction of mapped lines, we next sought additional insertion positions for lines that were not included in the agreement list. To do this, we generated additional suggested decodings by allowing two or more digital bits to differ between the codes derived from sequence reads and code words that were used in the pooling design but not yet reliably assigned to positions. The first of these lists consisted of suggested decodings where reads from more than one pool were expected by the code word but missing in the set of mapped sequence reads (creating a multiple zero-to-one error list, see *Materials and Methods* for details). The second of these lists included lines that were assigned to positions consisting of reads not only from the pools associated with the code word but also from other pools (creating a multiple one-to-zero error list). This latter list was designed to obtain suggested map positions in cases where multiple lines shared the same insertion position. Finally, we generated lists in which there was a mismatch between the suggested position and the chromosome determined during strain construction (creating a "chromosome error list"). These lists were then processed using the same quality criteria described above.

To assess the accuracy of these additional lists, we mapped 50 more lines by splinkerette PCR, focusing on lines that were not included in the agreement list (File S2). Comparing all of these error lists to this validation set revealed that many lines were correctly mapped, with accuracy ranging between 36.7% and 80%, depending on the list (Table 2). Among these correct suggestions, we even found several instances in which we recovered the correct insertion position for multiple lines where the transposable element had targeted exactly the same genomic site in the same orientation (Figure S2). Thus, in some instances, our analysis was able to separate mixed codes.

Our analysis generated map positions for 761/1065 (71.5%) of lines with a measured accuracy of 100%, as well as map positions for an additional 179/1065 (16.8%) of lines with an accuracy of between 69.2% and 90.9% (Table 2), representing 88.5% of the collection in aggregate.

In addition, for lines that were not mapped with 100% accuracy, by additional data processing, we generated 692 partially overlapping suggested map positions, which have lower confidence (26.8–66.7%, based on all splinkerette mapping data, Table 2). In total, this analysis generated map position suggestions for 1060/1065 lines (99.5% of the collection; Table 2 and Table S3). We note that the list of suggested map positions can be further refined by prioritizing suggestions on lists with higher accuracy, suggestions with higher scores, suggestions in which the 5′ and 3′ datasets agree, or by using machine-learning methods to identify position features reflective of accuracy.

Discussion

Here we describe how the sequencing efficiencies associated with NGS technology can be combined with a directed pooling strategy to efficiently map large numbers of transposon insertion sites in a multicellular genetic model organism. Using this approach, we mapped a collection of >1000 independent insertions, obtaining 88.5% coverage with high confidence. Digital encoding of the samples allowed for the identities of >1000 samples to be encoded in 15 pools, representing an ~70-fold reduction in time and reagent costs associated with sample processing and an ~5-fold reduction in per sample sequencing costs, a difference that will continue to grow as the cost of NGS continues to fall.

While our current approach succeeded, we note that several simple improvements are possible. For instance, since the p7-side Illumina adapter is added to the end of the primer during transposon amplification, omitting the p7-side adapter from the initial adapter ligation and/or performing nested PCR could dramatically reduce the number of non-transposon reads. In addition, limiting the pool of used Hamming code words to those with high entropy, or increasing the Hamming distance between used code words, would facilitate decoding. That is, using code words that contain comparable numbers of digital 1s and 0s, as well as using code word libraries that require several errors to convert a code word used for one line into a code used for another line, would make decoding simpler. Nonetheless, our approach reduces the workload associated with mapping large numbers of insertions, reducing the number of reactions necessary to map nearly 1000 insertions to 15 samples and requiring only a simple set of barcodes necessary to define this small group of pools. The 15 pools that were required to encode 1000 lines using our method represent roughly half the number of pools that would be needed for either a plate/row/column pooling scheme (which scales roughly linearly with sample size) or using DNA Sudoku (which scales as a function of the square root of the number of samples) (Erlich *et al.* 2009). Using Hamming codes, the number of additional samples that can be encoded scales roughly as a factor of 2^n, where n is the number of pools, allowing large numbers of additional samples to be encoded by a small increase in pool number. Thus, the scale of the pooling strategy can be readily adapted to the scale of the library to be mapped and offers larger and larger increases in efficiency as the number of lines grows. Finally, we note that this approach is not, by design, limited to the sequencing of insertion fragments, but rather can be extended to multiplex the sequencing of any collection of different DNA fragments.

Acknowledgments

We thank Yvette Fisher, Jonathan Leong, and Samuel Lasse for helpful discussions; the Stanford Functional Genomics Facility, particularly Xuhuai Ji and Vanita Natu, for experimental advice and assistance; and Xiaojing Gao, Jessica Tsai, Mya Win, and Wes Grueber for contributing splinkerette mapping data. We thank Jennifer Esch, Yvette Fisher, Xiaojing Gao, Tina Schwabe, and Helen Yang for comments on the manuscript. D.M.G was supported by a Ruth L. Kirschstein National Research Service Award postdoctoral fellowship (F32 EY020040) from the National Eye Institute. L.F. was supported by a Fulbright International Science and Technology scholarship and a Bio-X Stanford Interdisciplinary graduate fellowship (Bruce and Elizabeth Dunlevie fellow). M.S. was supported by a postdoctoral fellowship from the Jane Coffin Childs Memorial Fund for Medical Research. This work was funded by a National Institutes of Health Director's Pioneer award DP1 OD003530 (T.R.C.) and by R01 EY022638 (T.R.C).

Literature Cited

Barton, G. J., 1993 An efficient algorithm to locate all locally optimal alignments between two sequences allowing for gaps. Comput. Appl. Biosci. 9: 729–734.

Bellen, H. J., R. W. Levis, Y. He, J. W. Carlson, M. Evans-Holm *et al.*, 2011 The Drosophila gene disruption project: progress using transposons with distinctive site specificities. Genetics 188: 731–743.

Bentley, D. R., S. Balasubramanian, H. P. Swerdlow, G. P. Smith, J. Milton *et al.*, 2008 Accurate whole human genome sequencing using reversible terminator chemistry. Nature 456: 53–59.

Bire, S., and F. Rouleux-Bonnin, 2012 Transposable elements as tools for reshaping the genome: it is a huge world after all! Methods Mol. Biol. 859: 1–28.

Devon, R. S., D. J. Porteous, and A. J. Brookes, 1995 Splinkerettes–improved vectorettes for greater efficiency in PCR walking. Nucleic Acids Res. 23: 1644–1645.

Erlich, Y., K. Chang, A. Gordon, R. Ronen, O. Navon *et al.*, 2009 DNA Sudoku–harnessing high-throughput sequencing for multiplexed specimen analysis. Genome Res. 19: 1243–1253.

Febrer, M., K. McLay, M. Caccamo, K. B. Twomey, and R. P. Ryan, 2011 Advances in bacterial transcriptome and transposon insertion-site profiling using second-generation sequencing. Trends Biotechnol. 29: 586–594.

Gohl, D. M., M. A. Silies, X. J. Gao, S. Bhalerao, F. J. Luongo *et al.*, 2011 A versatile in vivo system for directed dissection of gene expression patterns. Nat. Methods 8: 231–237.

Golay, M. J. E., 1949 Notes on digital coding. Proceedings of the IRE 37: 657.

Goodman, A. L., N. P. McNulty, Y. Zhao, D. Leip, R. D. Mitra *et al.*, 2009 Identifying genetic determinants needed to establish a human gut symbiont in its habitat. Cell Host Microbe 6: 279–289.

Hamady, M., J. J. Walker, J. K. Harris, N. J. Gold, and R. Knight, 2008 Error-correcting barcoded primers for pyrosequencing hundreds of samples in multiplex. Nat. Methods 5: 235–237.

Hamming, R., 1950 Error detecting and error correcting codes. Syst Tech J XXIX: 147–160.

Iskow, R. C., M. T. McCabe, R. E. Mills, S. Torene, W. S. Pittard *et al.*, 2010 Natural mutagenesis of human genomes by endogenous retrotransposons. Cell 141: 1253–1261.

Langmead, B., C. Trapnell, M. Pop, and S. L. Salzberg, 2009 Ultrafast and memory-efficient alignment of short DNA sequences to the human genome. Genome Biol. 10: R25.

Mazurkiewicz, P., C. M. Tang, C. Boone, and D. W. Holden, 2006 Signature-tagged mutagenesis: barcoding mutants for genome-wide screens. Nat. Rev. Genet. 7: 929–939.

Meyer, M., and M. Kircher, 2010 Illumina sequencing library preparation for highly multiplexed target capture and sequencing. Cold Spring Harb. Protoc. (6): pdb prot5448.

Ochman, H., A. S. Gerber, and D. L. Hartl, 1988 Genetic applications of an inverse polymerase chain reaction. Genetics 120: 621–623.

Potter, C. J., and L. Luo, 2010 Splinkerette PCR for mapping transposable elements in Drosophila. PLoS ONE 5: e10168.

Prabhu, S., and I. Pe'er, 2009 Overlapping pools for high-throughput targeted resequencing. Genome Res. 19: 1254–1261.

Silies, M., D. M. Gohl, Y. E. Fisher, L. Freifeld, D. A. Clark *et al.*, 2013 Modular use of peripheral input channels tunes motion-detecting circuitry. Neuron 79: 111–127.

Uren, A. G., H. Mikkers, J. Kool, L. van der Weyden, A. H. Lund *et al.*, 2009 A high-throughput splinkerette-PCR method for the isolation and sequencing of retroviral insertion sites. Nat. Protoc. 4: 789–798.

Communicating editor: N. Perrimon

GENETICS

Supporting Information
http://www.genetics.org/lookup/suppl/doi:10.1534/genetics.113.159483/-/DC1

Large-Scale Mapping of Transposable Element Insertion Sites Using Digital Encoding of Sample Identity

Daryl M. Gohl, Limor Freifeld, Marion Silies, Jennifer J. Hwa, Mark Horowitz, and Thomas R. Clandinin

DOI: 10.1534/genetics.113.159483

a

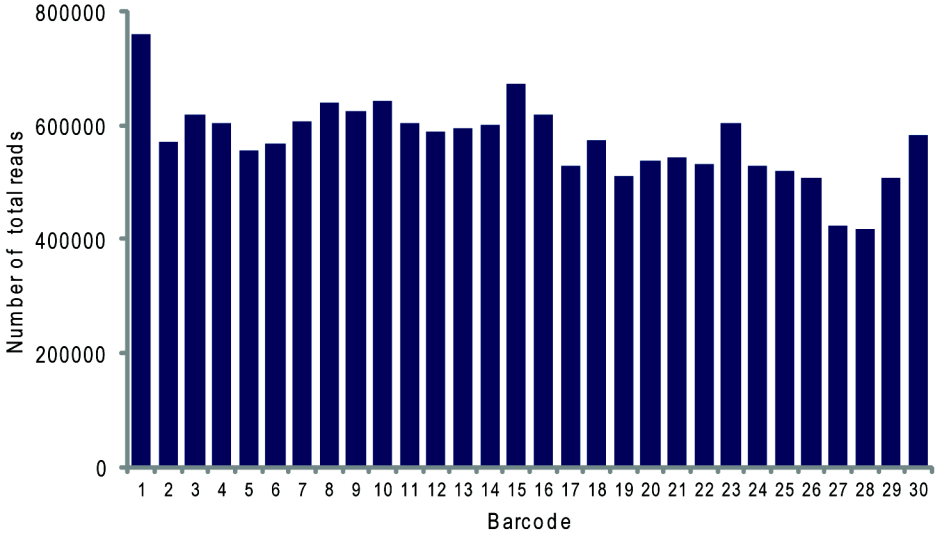
800000
600000
400000
200000
0
Number of total reads
1 2 3 4 5 6 7 8 9 10 11 12 13 14 15 16 17 18 19 20 21 22 23 24 25 26 27 28 29 30
Barcode

b

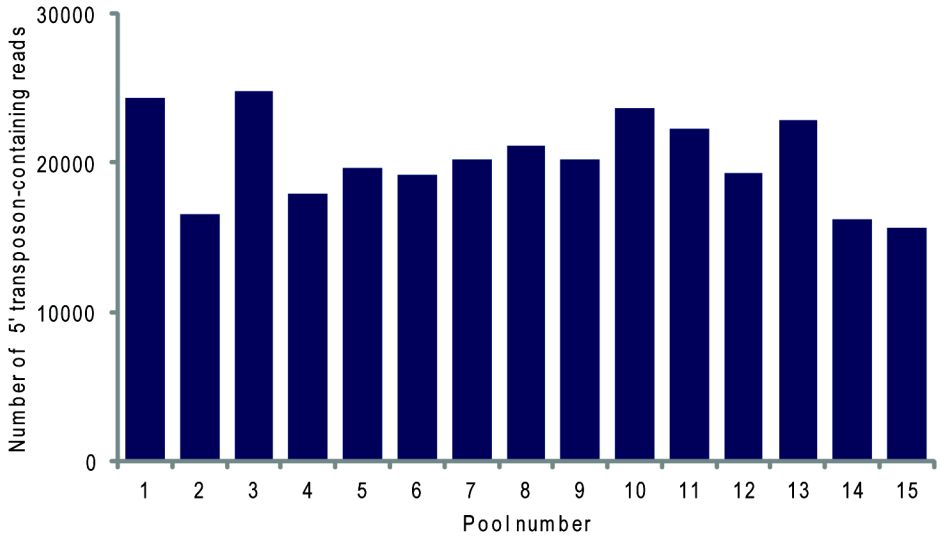
30000
20000
10000
0
Number of 5' transposon-containing reads
1 2 3 4 5 6 7 8 9 10 11 12 13 14 15
Pool number

c

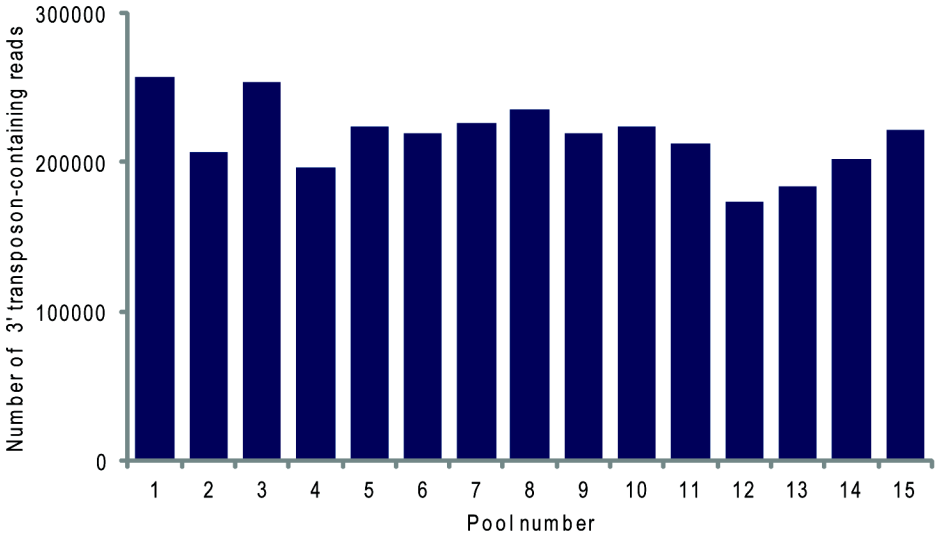
300000
200000
100000
0
Number of 3' transposon-containing reads
1 2 3 4 5 6 7 8 9 10 11 12 13 14 15
Pool number

Figure S1 Sequenced Read Statistics

Plot of the number of sequencing reads associated with each barcode (a) and the number of putative transposon-containing reads identified in each pool for the 5' *piggyBac* end (b) and the 3' *piggyBac* end (c).

a

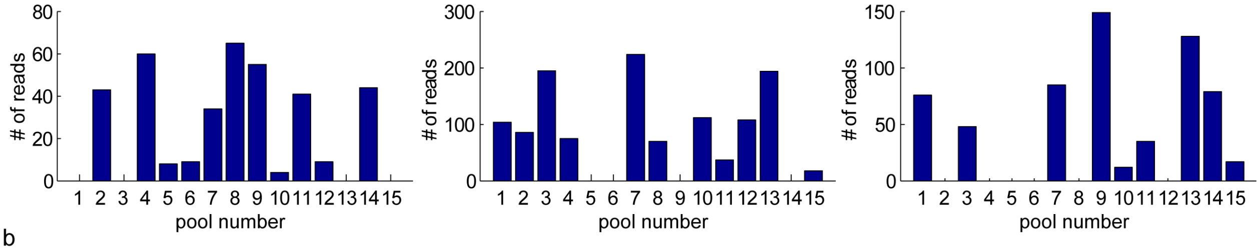

b

0102	0 1 0 1 1 1 1 1 1 0 0 0 0 1 0	0602	0 1 1 1 0 0 1 0 0 1 1 0 1 0 0	0888	0 0 1 0 0 0 0 0 1 1 0 0 1 1 1
0701	0 0 0 1 0 0 0 1 0 1 1 1 0 0 0	0735	1 0 1 0 0 0 1 1 0 1 0 1 1 0 1	0998	1 0 0 0 0 0 1 0 1 0 1 0 1 0 0
mixed	0 1 0 1 1 1 1 1 1 1 1 1 0 1 0	mixed	1 1 1 1 0 0 1 1 0 1 1 1 1 0 1	mixed	1 0 1 0 0 0 1 0 1 1 1 0 1 1 1

c

Line	Chrom. arm	Position	Score	UID	List ID
102	2L	11012283	5.160714	159	6
102	2L	11045687	2.178571	160	8
701	2L	11012283	2.3	1129	6
701	2L	11012287	2.4	1130	8

Line	Chrom. arm	Position	Score	UID	List ID
602	3R	11972317	7.321429	991	6
602	3R	11972321	6.303571	992	8
735	3R	11972317	6.875	1168	6
735	3R	11972321	3.875	1169	8

Line	Chrom. arm	Position	Score	UID	List ID
888	2L	16681913	5.055556	1369	6
888	2RHet	1425417	2.388889	1370	8
998	2L	16681913	6	1519	6
998	2L	16681909	4.6	1520	8

Figure S2 Identifying insertions in the same position with the same orientation

a) Distribution of reads in pools at three insertion positions that were unassigned in any of the agreement or single error-correction lists, but had suggestions in the multiple one-to-zero error lists.

b) The pools associated with the lines suggested by the multiple one-to-zero error lists at these positions and the expected codes resulting from mixtures of these pools.

c) For these three pairs of lines, 10 out of 12 map positions suggested by the multiple one-to-zero error lists (Table 2) were correct (highlighted in green). In these cases, correct mappings could be identified on the basis of their confidence score.

Files S1 and S2

Available for download at http://www.genetics.org/lookup/suppl/doi:10.1534/genetics.113.159483/-/DC1 as PDF files.

File S1 Splinkerette sequencing data for reference set

FASTA sequences for the 66 lines used to characterize the decoding algorithm.

File S2 Splinkerette sequencing data for validation set

FASTA sequences for the 50 lines used to validate and characterize the reliability of the non-agreement lists.

Tables S1-S3

Available for download at http://www.genetics.org/lookup/suppl/doi:10.1534/genetics.113.159483/-/DC1 as Excel files.

Table S1 List of the oligonucleotide sequences used in this study

For indexing primers, the DNA barcode sequence is in lowercase. * stands for a phosphorothiol modification at the indicated position.

Table S2 List of Hamming codes used for all lines

Table listing the line number, chromosomal location, ID number, and binary Hamming code word for each line.

Table S3 List of insertion sites, sequences, and metadata for all suggested line-position associations

Table columns are as follows. UID: Unique ID assigned to each suggestion. Line: Line number. line_chrom: Annotated chromosome of insertion. read_chrom: Chromosome arm of suggested map position. position: Map position of sequence (putative insertion site). Score 1.0: mean number of reads in 1 bins - mean number of reads in 0 bins. Score 2.0 (as described in main text): mean number of unique read lengths in 1 bins - mean number of unique read lengths in 0 bins. example sequence: One of the mapped sequence reads. Orientation: orientation of the putative transposon insertion ('+' = 5' to 3', '-' = 3' to 5'). List ID: List that the suggestion was drawn from (see Table 2). N different lines with the same insertion position. N reads: total number of reads in a given peak. N read containing pools: number of pools containing at least one read. N pools containing reads of a unique length only. mean read length. long sequence: longer read drawn from collection of reads mapping to a given position. long sequence primer: indicates whether the long sequence was drawn from a 5' (5) or 3' (3) pool. long seq.: Gene inserted in: BLAST result, if inserted within an intragenic region. long seq.: 5' gene and long seq.: 3' gene: BLAST result indicating the upstream and downstream gene if sequence maps to an intergenic region. correct: '1' indicates a match between the suggested decoding and a splinkerette sequence from either the reference or validation set. error: '1' indicates a mismatch between the suggested decoding and a splinkerette sequence from either the reference or validation set.